Theory and Modeling of Self-Organization and Propagation of Filamentary Plasma Arrays in Microwave Breakdown at Atmospheric Pressure

Jean-Pierre Boeuf,[1,2] Bhaskar Chaudhury,[1] and Guo Qiang Zhu[1]

[1]*Université de Toulouse; UPS, INPT; LAPLACE (Laboratoire Plasma et Conversion d'Energie); 118 route de Narbonne, F-31062 Toulouse cedex 9, France*

[2]*CNRS; LAPLACE; F-31062 Toulouse, France*

(Received 19 August 2009; revised manuscript received 10 December 2009; published 6 January 2010)

High power microwave breakdown at atmospheric pressure leads to the formation of filamentary plasma arrays that propagate toward the source. A two-dimensional model coupling Maxwell equations with plasma fluid equations is used to describe the formation of patterns under conditions similar to recent experiments and for a wave electric field perpendicular to the simulation domain or in the simulation domain. The calculated patterns are in excellent qualitative agreement with the experiments, with good quantitative agreement of the propagation speed of the filaments. The propagation of the plasma filaments is due to the combination of diffusion and ionization. Emphasis is put on the fact that free electron diffusion (and not ambipolar diffusion) associated with ionization is responsible for the propagation of the front.

DOI: 10.1103/PhysRevLett.104.015002 PACS numbers: 52.80.Pi, 51.50.+v, 52.38.Hb, 52.40.Db

Gas breakdown by microwave fields has been the subject of many experimental and theoretical works since the 1950s and a summary of the early work can be found in [1]. The studies of microwave breakdown have long been focused on the measurements and theoretical determination of the breakdown field as a function of pressure and pulse duration. The availability of fast camera and imaging systems has more recently allowed very interesting studies of the dynamics of microwave breakdown [2–7]. Some of these studies have shown the formation of complex plasma structures evolving in time and, under certain conditions, propagating toward the source. In this Letter we focus on the experimental results of Hidaka *et al.* [5,6] where accurate measurements and observations of the plasma dynamics and pattern formation during microwave breakdown are reported for different gases at and around atmospheric pressure. A model of these experiments has been recently proposed by Nam and Verboncoeur [8]. The model of [8] is one dimensional (1D) and is based on a fluid description of electron transport in argon at atmospheric pressure, assuming quasineutrality and ambipolar diffusion, coupled with the electromagnetic wave. The authors of [8] show that under these model assumptions, the incident wave is reflected by the forming filament (plasma sheets in the 1D model), resulting in an enhanced electric field at a distance of a quarter wavelength, $\lambda/4$ from the filament. Diffusion and ionization in the enhanced field leads to the formation of a new filament upstream, at a distance around $\lambda/4$ of the previous one. This is qualitatively consistent with the experimental observations and interpretations of [5,6]. The plasma density calculated in [8], however, reaches surprisingly high values (4.5×10^{23} m^{-3}), for an applied field amplitude of 5 MV/m at 110 GHz in argon at atmospheric pressure.

In this Letter we present a two-dimensional model of the propagation of a self-organized plasma array in conditions closer to those of [5], i.e., in air at atmospheric pressure. The model results are in excellent qualitative agreement with the experimental results of [5,6] and can explain the observed 3D structures. They give a good quantitative prediction of the propagation speed of the plasma pattern and show that free electron diffusion combined with ionization are responsible for the propagation of the plasma front (contrary to the model of [8] where the use of ambipolar diffusion leads to a large overestimation of the plasma density).

Before going into the details of the microwave breakdown model and results we first discuss the question of free vs ambipolar diffusion of the plasma front. In a microwave plasma, the total electric field is the sum of the high frequency wave field and of a dc or slowly varying field due to space charge effects. The high frequency field E plays an essential role in electron heating and ionization, but its contribution to particle transport averaged over one period of the wave is negligible. The field contributing to charged particle transport averaged over one cycle is the space charge field, E_{sp}, which should be obtained by solving Poisson's equation together with electron and ion transport equations. Under conditions where the plasma dimensions are much larger than the electron Debye length $\lambda_D = [\varepsilon_0 kT_e/e^2 n]^{1/2}$, it is often sufficient to describe space charge effects through an ambipolar diffusion coefficient D_a, and to write the continuity equation for the plasma density n, as:

$$\partial_t n - D\Delta n = S = n\nu_i. \quad (1)$$

Here, $D = D_a$ if one assumes ambipolar diffusion, S is the source term, ν_i is the ionization frequency and depends on

the wave field. For a constant, given, ionization frequency, the well known asymptotic solution of Eq. (1) is a Gaussian of the form:

$$n(\boldsymbol{r}, t) = At^{-3/2} \exp[\nu_i t - r^2/4Dt]. \quad (2)$$

The density of Eq. (2) exhibits a front that propagates at a speed $v = 2\sqrt{D\nu_i}$, and this result can be generalized [9] to more complex source terms S, for example, including electron-ion recombination, (with coefficient r_{ei}), i.e., such as $S = n\nu_i - r_{ei}n^2$. The characteristic length of the front, defined as $|\nabla n/n|^{-1}$ in a reference frame moving at the speed v, is $L = \sqrt{D/\nu_i}$.

The question is, however, should the diffusion coefficient in Eq. (1) be the ambipolar diffusion coefficient or the free electron diffusion coefficient? This question arises since even if the plasma dimension is much longer than the Debye length, the plasma density at the front goes to zero and, therefore, there should be a small region in the front where the electrons diffuse freely. This question has been considered somewhat empirically in several papers such as [2,10,11]. For example, in [2], the authors indicate that the calculated plasma propagation speed matches the experimental one only if the free diffusion coefficient is used in (1). Theoretical evidence of the fact that the free diffusion coefficient should be used has been provided by Ebert *et al.* in [12,13]. Ebert *et al.* consider streamer propagation under a dc electric field. They show that the velocity of the streamer front is equal to the electron drift velocity at the front, plus a corrective term due to diffusion and equal to $2\sqrt{D_e\nu_i}$ where D_e is the free electron diffusion. This result can certainly be applied to our problem where the cycle averaged electron drift velocity is zero, and the speed of the front is therefore $2\sqrt{D_e\nu_i}$. However, free diffusion prevails only in the front while the plasma bulk is controlled by ambipolar diffusion. A simple scaling parameter controlling the transition from ambipolar to free diffusion in the front can be deduced from the current continuity equation in the drift-diffusion approximation in the case of a planar front (similar to Eq. (5) of Ref [12]), which writes, assuming quasineutrality:

$$\tau_M \partial_t E_{sp} + E_{sp} = -\frac{D_e - D_i}{\mu_e + \mu_i} \frac{\partial_x n}{n}. \quad (3)$$

E_{sp} is the space charge field, τ_M is the dielectric (or Maxwell) relaxation time, $\tau_M = \varepsilon_0/[en(\mu_e + \mu_i)]$, ($\mu_e$, μ_i) and (D_e, D_i) are, respectively, the electron and ion mobility and diffusion coefficients. In a reference frame X moving with the front at the velocity $v = 2\sqrt{D_e\nu_i}$ the first term of the left-hand side of Eq. (3) is $\tau_M \partial_t E_{sp} = -v\tau_M \partial_X E_{sp}$ [13]. Approximating $\partial_X E_{sp}$ in the front by $-E_{sp}/2L$, where $L = \sqrt{D_e/\nu_i}$, we get $\tau_M \partial_t E_{sp} \approx \nu_i \tau_M E_{sp}$; i.e., the first term of Eq. (3) is of the order of $\alpha = \nu_i\tau_M$ with respect to the second term. Equation (3) can therefore be approximated by:

$$E_{sp} \approx -\frac{1}{1+\alpha} \frac{D_e - D_i}{\mu_e + \mu_i} \frac{\partial_x n}{n}. \quad (4)$$

Using this expression of the field in the electron flux $\Gamma = -n\mu_e E - D_e \partial_x n$, leads to $\Gamma \approx -D_{\text{eff}} \partial_x n$ with

$$D_{\text{eff}} \approx \frac{\alpha D_e + D_a}{\alpha + 1} \quad \text{with} \quad \alpha = \nu_i \tau_M = \lambda_D^2/L^2 \quad (5)$$

where we have assumed $\mu_i \ll \mu_e$, $D_i \ll D_e$.

The heuristic arguments above justify the use of Eq. (1) with the effective diffusion coefficient (5). This model is not mathematically exact but gives the good limits and a correct estimation of the parameter α controlling the crossover from ambipolar diffusion in the plasma ($\alpha \ll 1$) to free diffusion in the front ($\alpha \approx$ or > 1). Comparisons between numerical solutions of the drift-diffusion Poisson system for a given ionization frequency, with solutions of Eq. (1) with $D = D_{\text{eff}}$ show excellent agreement and will be presented in a forthcoming paper.

In our microwave problem we can expect that $v = 2\sqrt{D_e\nu_i}$ is still a good estimation of the front velocity, but with ν_i being the result of the complex interaction between the plasma and the wave. We now consider the coupling of Maxwell's equations with the plasma in air. Ionization and attachment are considered, but the effects of negative ions are neglected. Maxwell's equations:

$$\boldsymbol{\nabla} \times \boldsymbol{E} = -\partial_t \boldsymbol{B} \quad (6)$$

$$\boldsymbol{\nabla} \times \boldsymbol{H} = \boldsymbol{J} + \varepsilon_0 \partial_t \boldsymbol{E} \quad (7)$$

are coupled with the plasma equations through the electron current (ion current is neglected), $\boldsymbol{J} = -en\mathbf{v}_e$, with:

$$\partial_t \mathbf{v}_e = -e\boldsymbol{E}/m - \nu_m \mathbf{v}_e \quad (8)$$

$$\partial_t n - D_{\text{eff}} \Delta n = n(\nu_i - \nu_a) - r_{ei} n^2. \quad (9)$$

We use the classical assumption that the ionization and attachment frequencies ν_i and ν_a are functions (obtained from Bolsig+ [14]) of the local effective field E_{eff}:

$$E_{\text{eff}} = E_{\text{rms}}(1 + \omega^2/\nu_m^2)^{-1/2}. \quad (10)$$

Mobility, diffusion and recombination coefficients are supposed to be constant and given by $\mu_e = e(m\nu_m)^{-1} = 3.7 \times 10^{-2}$ m^2/V/s, $\mu_e/\mu_i = 200$, $D_e = \mu_e kT_e/e$, $D_i = 0$, $kT_e = 2$ eV, $r_{ei} = 0$. ν_m is the electron-neutral momentum transfer frequency.

Maxwell's equations are solved using the classical FDTD (finite-difference time-domain) numerical scheme with absorbing boundary conditions on the walls. After integration of the Maxwell equations over one cycle of the microwave field, the local effective field (10) is calculated and used to solve the quasineutral plasma density equation (9) for the next cycle [the time step of the density equation (9) is one cycle of the microwave field].

Maxwell's Eqs. (6) and (7) are then integrated together with Eq. (8) for another cycle, using the updated density. The spatial grids for Maxwell's equation and the density equation are different, because of the sharpness of the plasma front (respectively 100 and 500 grid points per wavelength). The amplitude of the incident field is 6 MV/m, the frequency is 110 GHz. The initial electron density is a Gaussian with maximum density 10^{13} m^{-3} and standard deviation 50 μm. The equations are solved in a 2D (x, y) Cartesian domain of dimensions ($3\lambda \times 3\lambda$) (invariance assumed in the direction perpendicular to the domain).

We consider two different simulation cases. In the first case, the electric field is perpendicular to the simulation domain and the magnetic field is in the domain, while the opposite is true in the second case. We see below that these two 2D simulations reproduce well the experimental (3D) patterns observed in the B and E planes of the incident wave.

Figure 1 shows the plasma density and rms field at three different times for the case of an E field perpendicular to the simulation domain. At $t = 106$ ns [Figs. 1(a) and 1(d)], a filamentary pattern has already formed (filaments are parallel to E, i.e., perpendicular to the simulation domain) and is propagating toward the source ($x = -\infty$). The mechanisms of pattern formation and propagation can be understood from Fig. 1. The filament at the front [Figs. 1(a) and 1(d) $t = 106$ ns] reflects and scatters the electromagnetic field. The resulting standing wave presents off-axis field maxima that generate two off-axis filaments [Figs. 1(b) and 1(e), $t = 118$ ns] through a combination of diffusion and ionization in the enhanced field. The addition of the field reflected by this structure to the incident field leads to a field maximum on axis, resulting in a new on-axis filament [Figs. 1(c) and 1(f), $t = 124$ ns].

The distance between on-axis filaments is on the order of $\lambda/4$ ($\lambda \sim 2.7$ mm). The electron density in the filaments reaches maximum values on the order of 3×10^{21} m^{-3}, significantly smaller than in [8]. The wave is only partially reflected by the filamentary pattern as seen on the 1D plots of Fig. 1. The front of the foremost filament therefore "sees" a field on the order of 5 MV/m. The ionization frequency for this field is about 2×10^9 s^{-1} and an estimation of the front velocity $2\sqrt{D_e \nu_i}$ for these conditions is 30 km/s, in agreement with the velocity that can be deduced from the simulated pattern propagation, and close to the measured values of [5,6]. The results also show that the propagation velocity is not sensitive to the value of the recombination coefficient. The details of the pattern may however depend on the value of the recombination coefficient. This will be discussed in a forthcoming paper. Note that in [8], where D_a was used instead of D_e in the front, the calculations were done for argon whose ionization frequency is considerably larger than in air. The higher value of ν_i compensates for the low value of D_a, so that the propagation speed in [8] seems of the same order of magnitude as in the experiments in air.

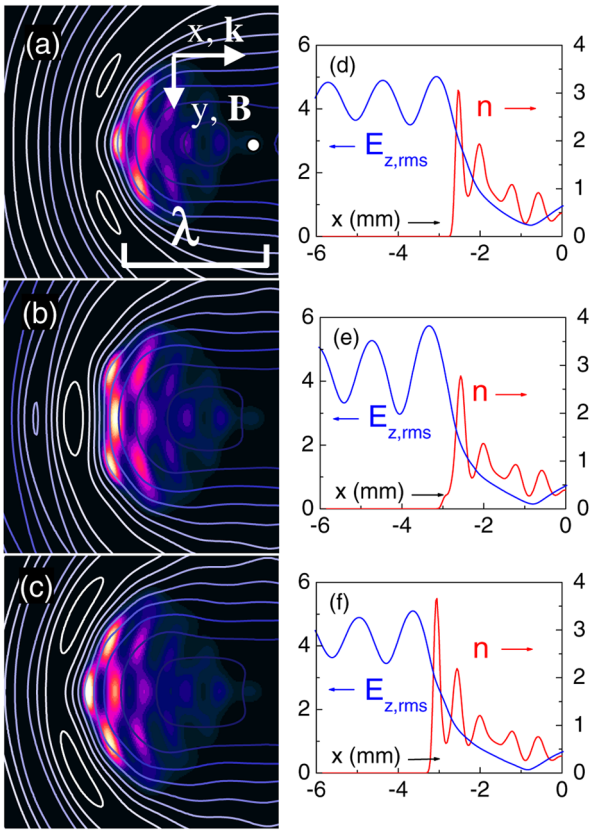

FIG. 1 (color online). (a),(b),(c) Distribution of the plasma density (filled contours, larger densities in lighter colors) and rms field (contour lines, higher field intensity corresponds to lighter color contours), $E_{z,\mathrm{rms}}(x, y)$ at three different times (respectively, 106, 118, and 124 ns) for a 6 MV/m wave amplitude at 110 GHz with an E field perpendicular to the simulation plane. The position of the initial Gaussian density is marked by a white dot in (a) [$x = 0$ in (d), (e), (f)]. The aspect ratio of the figures is 1; (d),(e),(f), density and rms field distributions on axis at the same times (units are 10^{21} m^{-3}, and MV/m, respectively). The wave propagates from left to right (wave vector $\mathbf{k} \parallel$ to the x direction). The magnetic field B of the incident wave is $\parallel$ to the y direction.

Results for the case where the E field is in the simulation plane are illustrated in Fig. 2. The filaments are stretched in the direction of the incident field. The initial Gaussian electron distribution first grows isotropically [Fig. 2(a), $t = 10$ ns]. When the plasma density becomes sufficiently large, the electric field is enhanced at the poles of the plasma ball in the direction of the applied field. Ionization increases in these regions and the plasma therefore propagates faster in the direction of the field [Fig. 2(a), $t = 20$ ns], forming an elongated filament in the y direction, sometimes called a microwave streamer. As the plasma density grows, the incident field starts to be reflected by the filament, giving rise, through a combination of ionization and diffusion, to standing waves and to the

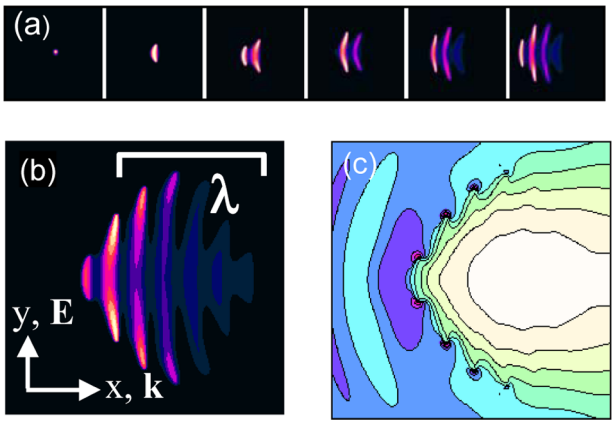

FIG. 2 (color online). (a) Evolution of the plasma density distribution for an E field in the simulation plane (6 MV/m, 110 GHz), at times $t = 10$, 20, 30, 40, 50, 60 ns (maximum plasma density, respectively, 6×10^{-2}, 3.2, 3.9, 4.9, 6.1, and 5.2×10^{21} m^{-3}, larger densities are in lighter colors); (b) Plasma density distribution at $t = 102$ ns (maximum 5.2×10^{21} m^{-3}); (c) rms field, $E_{\mathrm{rms}}(x, y) = \sqrt{E_{x,\mathrm{rms}}^2 + E_{y,\mathrm{rms}}^2}$ at $t = 102$ ns (maximum 6.7 MV/m, smaller fields are in lighter colors). The wave propagates from left to right (wave vector $\mathbf{k} \parallel$ to the x direction). The electric field E of the incident wave is $\parallel$ to the y direction.

generation of a new filament upstream, at a distance about $\lambda/4$ from the previous one [Fig. 2(a), $t = 30$ ns]. The propagation of the plasma toward the source is therefore associated with the reflection and formation of standing waves. The elongation of the plasma filaments in the direction parallel to the incident field is associated with the field enhancement at the tip of each filament. The filament growth stops because of the screening of the field by the new filaments. Figure 2(b) is in excellent qualitative agreement with images of the plasma in the E plane obtained in [5,6]. The standing wave in front of the plasma pattern and the enhanced field at the tip of each filament can be clearly seen in Fig. 2(c).

In summary, a 2D model coupling Maxwell's equations and a simple plasma diffusion equation at atmospheric pressure can reproduce strikingly well the features observed during microwave breakdown at atmospheric pressure. Two 2D simulations performed for a transverse electric and a transverse magnetic wave reproduce the experimental 3D patterns observed in the B and E planes of the incident wave. The propagation of the filamentary plasma pattern toward the source is due to an ionization wave mechanism driven by a combination of diffusion and ionization in the E field pattern resulting from reflection and scattering of the wave by the filaments. Free electron diffusion and not ambipolar diffusion (used in many modeling works) must be taken into account to describe the propagation of the plasma front. Filaments develop and extend in the direction of the incident E due to field enhancement by polarization at their tip. A pattern of parallel filaments distant from about $\lambda/4$ is formed and propagates toward the source. The propagation speed is on the order of $2\sqrt{D_e \nu_i}$ where the ionization frequency is the ionization rate at the front. Calculations performed for different gases and pressures also show good agreement with the experimental results of Ref. [6] and will be presented in future papers.

This work has been performed in the frame of the RTRA STAE PLASMAX project.

[1] A. D. MacDonald, *Microwave Breakdown in Gases* (John Wiley & Sons, New York, 1966).
[2] A. L. Vikharev, A. M. Gorbachev, A. V. Kim, and A. L. Kolsyko, Sov. J. Plasma Phys. **18**, 554 (1992).
[3] S. Popović, R. J. Exton, and G. C. Herring, Appl. Phys. Lett. **87**, 061502 (2005).
[4] I. I. Esakov, L. P. Grachev, K. V. Khodataev, V. L. Bychkov, and D. M. Van Wie, IEEE Trans. Plasma Sci. **35**, 1658 (2007).
[5] Y. Hidaka, E. M. Choi, I. Mastovsky, M. A. Shapiro, J. R. Sirigiri, and R. J. Temkin, Phys. Rev. Lett. **100**, 035003 (2008).
[6] Y. Hidaka, E. M. Choi, I. Mastovsky, M. A. Shapiro, J. R. Sirigiri, R. J. Temkin, G. F. Edmiston, A. A. Neuber, and Y. Oda, Phys. Plasmas **16**, 055702 (2009).
[7] R. P. Cardoso, T. Belmonte, C. Noël, F. Kosior, and G. Henrion, J. Appl. Phys. **105**, 093306 (2009).
[8] S. K. Nam and J. P. Verboncoeur, Phys. Rev. Lett. **103**, 055004 (2009).
[9] U. Ebert and W. van Saarloos, Physica (Amsterdam) **146D**, 1 (2000).
[10] O. I. Voskoboiikova, S. L. Ginzburg, V. F. D'Yachenko, and K. V. Khodataev, Tech. Phys. **47**, 955 (2002).
[11] J. T. Mayhan, R. L. Fante, R. Elkin, J. Klugerman, and J. Yos, J. Appl. Phys. **42**, 5362 (1971).
[12] U. Ebert, W. van Saarloos, and C. Caroli, Phys. Rev. Lett. **77**, 4178 (1996).
[13] U. Ebert, W. van Saarloos, and C. Caroli, Phys. Rev. E **55**, 1530 (1997).
[14] G. J. M. Hagelaar and L. C. Pitchford, Plasma Sources Sci. Technol. **14**, 722 (2005).